DOI: 10.1002/chem.201001297

VIP

Hydrogen-Atom Abstraction from Methane by Stoichiometric Vanadium–Silicon Heteronuclear Oxide Cluster Cations

Xun-Lei Ding,[a] Yan-Xia Zhao,[a, b] Xiao-Nan Wu,[a, b] Zhe-Chen Wang,[a, b] Jia-Bi Ma,[a, b] and Sheng-Gui He*[a]

Abstract: Vanadium–silicon heteronuclear oxide cluster cations were prepared by laser ablation of a V/Si mixed sample in an O_2 background. Reactions of the heteronuclear oxide cations with methane in a fast-flow reactor were studied with a time-of-flight (TOF) mass spectrometer to detect the cluster distribution before and after the reactions. Hydrogen abstraction reactions were identified over stoichiometric cluster cations $[(V_2O_5)_n(SiO_2)_m]^+$ ($n=1$, $m=1$–4; $n=2$, $m=1$), and the estimated first-order rate constants for the reactions were close to that of the homonuclear oxide cluster $V_4O_{10}^+$ with methane. Density functional calculations were performed to study the structural, bonding, electronic, and reactivity properties of these stoichiometric oxide clusters. Terminal-oxygen-centered radicals ($O_t^{\bullet}$) were found in all of the stable isomers. These $O_t^{\bullet}$ radicals are active sites of the clusters in reaction with CH_4. The $O_t^{\bullet}$ radicals in $[V_2O_5(SiO_2)_{1-4}]^+$ clusters are bonded with Si rather than V atoms. All the hydrogen abstraction reactions are favorable both thermodynamically and kinetically. This work reveals the unique properties of metal/nonmetal heteronuclear oxide clusters, and may provide new insights into CH_4 activation on silica-supported vanadium oxide catalysts.

Keywords: C–H activation · cluster compounds · density functional calculations · mass spectrometry · methane activation · radicals

Introduction

As one of the "holy grails" in chemistry, the activation of methane has been studied for many decades because it may enable the conversion of cheap and abundant natural gas into much more valuable organic compounds.[1–3] Due to the extremely high stability of methane, high temperature (>700 °C) is necessary to achieve high CH_4 conversion efficiency and selectivity, and undesirable byproducts are always produced in traditional catalytic processes.[4]

Gas-phase studies on the low-temperature activation of methane (or other alkanes) by clusters have attracted much interest, partly due to the possibility of revealing the mechanisms for reactions occurring on catalyst surfaces.[5–25] In these studies, CH_4 is found to be able to lose one H atom to generate the $CH_3^{\bullet}$ radical over some reactive clusters under ambient conditions. Note that the generation of $CH_3^{\bullet}$ from CH_4 is also considered to be the key step in the oxidative dehydrogenation and dimerization of methane in condensed phase studies.[26–30] Apart from metal ions (such as Au_2^+)[5–7] and metal–ligand ions (such as $[PtL]^+$),[8–12] many oxide cations, such as TiO_2^+,[13] ZrO_2^+,[13] MoO_3^+,[14] FeO^+,[15] OsO_4^+,[16] $V_4O_{10}^+$,[17] MgO^+,[18] $(Al_2O_3)_{3-5}^+$,[19–20] SO_2^+,[21] and $P_4O_{10}^+$,[22] were found to be capable of abstracting one H atom from CH_4 at room temperature (RT), and the oxygen-centered radical (denoted as $O^{\bullet}$) in these clusters (also over the condensed phase catalysts[31,32]) was suggested to play an important role in the reactions. In our recent experimental work,[33,34] a few series of stoichiometric transition metal oxide cations $M_xO_y^+$ ($2y-nx=0$, in which n is the number of valence electrons of M, and M = Ti, Zr, Hf, V, Nb, Ta, Mo, W, Re, or Ce) are found to activate the C–H bond of CH_4 under near-RT conditions. Our theoretical work[23] based on density functional theory (DFT) calculations sup-

[a] Dr. X.-L. Ding, Y.-X. Zhao, X.-N. Wu, Z.-C. Wang, J.-B. Ma, Prof. S.-G. He
Beijing National Laboratory for Molecular Science
State Key Laboratory for Structural Chemistry of Unstable and Stable Species
Institute of Chemistry, Chinese Academy of Sciences
Zhongguancun North First Street 2, Beijing, 100190 (P. R. China)
Fax: (+86) 10-62559373
E-mail: shengguihe@iccas.ac.cn

[b] Y.-X. Zhao, X.-N. Wu, Z.-C. Wang, J.-B. Ma
Graduate School of Chinese Academy of Sciences
Beijing 100039 (P. R. China)

Supporting information for this article is available on the WWW under http://dx.doi.org/10.1002/chem.201001297.

ported these findings, and further suggested that not only the cations but also the neutral and anionic clusters may have the character of O$^{\bullet}$ when the composition of cluster $M_xO_y^q$ satisfies the equation $\Delta \equiv 2y-nx+q=1$, in which q is the cluster charge number (0, ± 1). The above research has provided some insight into how methane may be activated by metal oxides at low temperature or relatively ambient conditions.

Practical catalysts are often made up of the active phase and a support material, such as V_2O_5/SiO_2. The interface structures and bonding properties between the support material and the active phase can greatly influence the reactivity.[35–37] Thus, in addition to the studies on homonuclear oxide clusters, it is necessary and interesting to investigate the structural and reactivity properties of heteronuclear oxide clusters $M_xN_yO_z^q$ (such as M=V, and N=Si),[23,38–42] which are investigated much less compared to the extensively studied homonuclear oxide clusters.[34,43–48]

Recently, the silica-supported vanadia system (VO_x/SiO_2) was found to display high catalytic performance in the selective oxidation of methane at relatively low temperature.[49,50] As an important type of catalyst for many reactions, VO_x/SiO_2 has been widely studied both experimentally and theoretically.[35,36,49–56] To reveal the catalytic mechanisms at the molecular level, we started to investigate the reactivity of $V_xSi_yO_z^{\pm 1,0}$ heteronuclear oxide clusters toward C–H activation of alkane molecules. This study focuses on the possible existence of radical oxygen centers in cationic $V_xSi_yO_z^+$ clusters, and their reactivity toward methane.

Results and Discussion

Cluster generation: To generate the V–Si heteronuclear oxide clusters, a V/Si mixed sample with a molar ratio of V:Si=1:1 is used as the target of laser ablation. Figure 1 presents a typical time-of-flight (TOF) mass spectrum for the distribution of $V_xSi_yO_z^+$ clusters generated under the conditions of 1% O_2 seeded in 5 atm He. The homonuclear oxide clusters $V_xO_z^+$ and $Si_yO_z^+$ are also generated in our experiment, and the signals of $V_xO_z^+$ are generally more intense than those of $Si_yO_z^+$. For the heteronuclear oxide clusters ($V_xSi_yO_z^+$, x, $y\neq 0$), stoichiometric clusters $[(V_2O_5)_n(SiO_2)_m]^+$ ($n=1$, $m=1$–4; $n=2$, $m=1$) are generated along with oxygen-poor or oxygen-rich $V_xSi_yO_z^+$ clusters. In Figure 1 the heteronuclear oxide clusters are classified into four series according to the number of V atoms: $VSi_{1-2}O_{2-9}$, $V_2Si_{1-4}O_{5-15}$, $V_3Si_{1-3}O_{11-14}$, and V_4SiO_{12-14}; these can be further classified into subseries according to the number of Si atoms. It should be noted that silicon has three stable isotopes: ^{28}Si (92.2%), ^{29}Si (4.7%), and ^{30}Si (3.1%), whereas V and O have only one dominant isotope each,[57] so on the high mass side of each main peak of $V_xSi_yO_z^+$, two minor peaks with a mass difference (Δ_{mass}) of +1 and +2 amu can be assigned as $V_x{}^{28}Si_{y-1}{}^{29}SiO_z^+$ and $V_x{}^{28}Si_{y-1}{}^{30}SiO_z^+$, respectively.

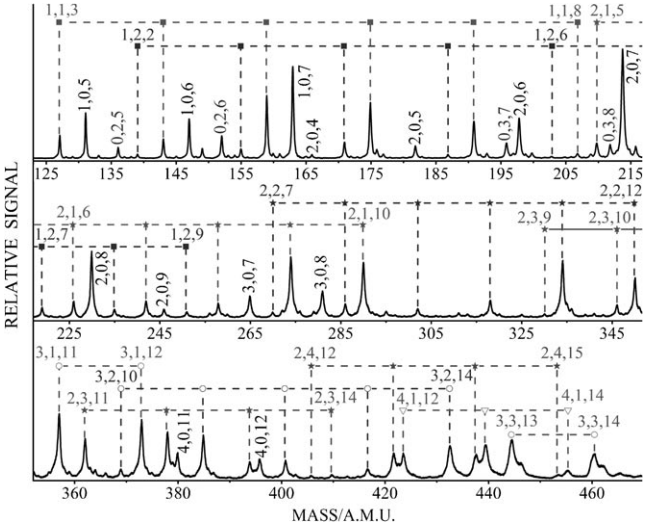

Figure 1. TOF mass spectra for the distribution of V–Si heteronuclear oxide cluster cations. $V_xSi_yO_z^+$ are denoted as x,y,z. Series with $x=1$, 2, 3, and 4 are marked by ■, *, ○, and ▽, respectively.

Reactions with CH_4: The TOF mass spectra for the reactions of $V_xSi_yO_z^+$ clusters with CH_4 and deuterated methane (CD_4) under near-RT conditions are plotted in Figure 2. After the reactions with CH_4 (Figure 2b), the peak intensities of the stoichiometric clusters $[(V_2O_5)_n(SiO_2)_m]^+$ ($n=1$, $m=1$–4; $n=2$, $m=0$, 1) decrease, and the signals at the positions of $\Delta_{mass}=+1$ amu increase simultaneously. This indicates that these stoichiometric cations may abstract one H atom from CH_4 to produce the hydroxide cationic clusters $[(V_2O_5)_n(SiO_2)_mH]^+$ and a neutral methyl radical, as shown in Equation (1).

$$[(V_2O_5)_n(SiO_2)_m]^+ + CH_4 \rightarrow [(V_2O_5)_n(SiO_2)_mH]^+ + CH_3 \quad (n=1,\ m=1-4;\ n=2,\ m=0,\ 1) \tag{1}$$

This reaction is further confirmed by isotopic labeling experiments with CD_4. In Figure 2c, signals at the positions of $\Delta_{mass}=+2$ amu increase if CD_4 is used instead of CH_4. The H abstraction reaction is also observed for $V_2Si_2O_{11}^+$, which can be viewed as the stoichiometric $V_2Si_2O_9^+$ cluster associated with one O_2 molecule.

Note that the association products $V_xSi_yO_zCH_4^+$ can only be well assigned in the D-labeled spectra. For example, $V_2SiO_{7,8}CD_4^+$ can be identified in Figure 2c1, and the peaks of the hydrogen species $V_2O_{7,8}CH_4^+$ are overlapped with those of $V_2SiO_{8,9}^+$. The association product $V_2SiO_7HCH_4^+$ is also found in our experiments, and the corresponding signal increase due to isotopic $V_2SiO_7DCD_4^+$ can be identified in the D-labeled spectra. The signal increase attributed to $V_2SiO_7HCH_4^+$ cannot be assigned to $V_2SiO_8H^+$, because the evidence of $V_2SiO_8D^+$ formation is not apparent, whereas the intense signal of $V_2SiO_8CD_4^+$ is observed (corresponding to the reduction of the $V_2SiO_8^+$ peak). Our results indicate that $V_2SiO_7^+$ (and also $V_2Si_2O_9^+$) may activate CH_4

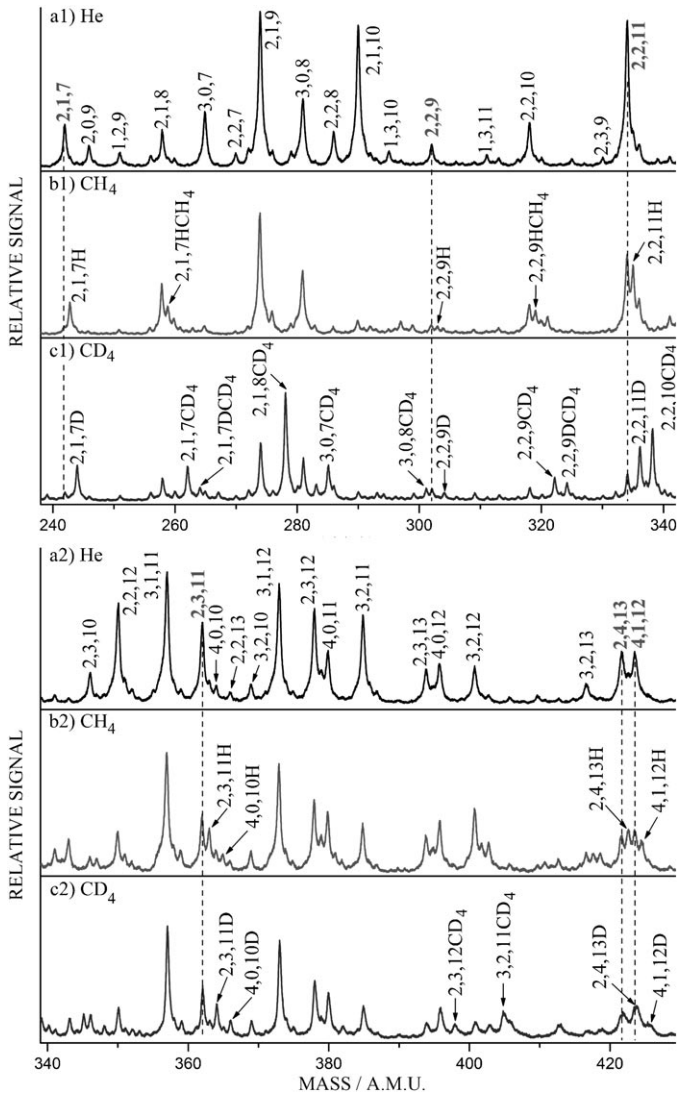

Figure 2. TOF mass spectra for reactions of $V_xSi_yO_z^+$ clusters with a) He gas (for reference), b) 0.6 Pa CH_4, and c) 0.6 Pa CD_4. Numbers *x*,*y*,*z* denote $V_xSi_yO_z^+$.

not only before but also after the association with another CH_4 molecule (note that $V_2SiO_7CD_4^+$ is observed in Figure 2c1).

The first-order rate constant k_1 of the H abstraction reaction in the fast-flow reactor can be estimated by $I=I_0\exp(-k_1\rho l/v)$, in which I and I_0 are the signal magnitudes of the $V_xSi_yO_z^+$ cluster in the presence and absence of reagent gas CH_4, respectively, ρ is the molecular density of the reactant gas,[58] l is the effective path length of the reactor ($\approx$60 mm), and v is the cluster beam velocity ($\approx 1\ km\,s^{-1}$). The estimated rate constants of the reactions of $V_2SiO_7^+$, $V_2Si_2O_9^+$, $V_2Si_3O_{11}^+$, $V_2Si_4O_{13}^+$, and $V_4SiO_{12}^+$ with CH_4 are 2.9×10^{-10}, 1.1×10^{-10}, 6.6×10^{-11}, 2.0×10^{-11}, and $1.5\times10^{-11}\ cm^3\,molecule^{-1}\,s^{-1}$, respectively. The relative uncertainties for the rate constants reported in this work are estimated to be about 20%, whereas the uncertainties for the absolute k_1 values can be large (50–80%) due to the systematic deviations in determining the molecular density of CH_4 (ρ) and the reaction time (l/v).[58] A note in reference [59] provides some discussion on the absolute rate constants measured with different experiments.[13,17,33,34,60] It should be pointed out that, with the experimental uncertainties, the relative k_1 values decrease with m for the four stoichiometric clusters $[(V_2O_5)(SiO_2)_m]^+$ with $m=1$–4, and k_1 for $V_4SiO_{12}^+ + CH_4$ is the smallest. The reason may be rationalized based on the computational results below.

Most stable structures of $[(V_2O_5)_n(SiO_2)_m]^+$ clusters and the interpretation of experimental reactivity: To verify the reactivity of $[(V_2O_5)_n(SiO_2)_m]^+$ ($n=1$, $m=1$–4; $n=2$, $m=1$) toward CH_4, theoretical calculations are performed on these clusters to find the stable isomers and especially the locations of the spin densities (or radicals for short) in these clusters. The lowest energy isomers for each cluster are plotted in Figure 3. Information about the bond lengths of V–O_t and Si–O_t and the distributions of Mulliken spin densities is also given (O_t indicates a terminal oxygen atom).

In the most stable isomer of $V_2SiO_7^+$ (I01), radicals are localized on one O_t atom bonded to the Si atom, and the Mulliken spin density is 0.97 |e|. The calculated Wiberg bond order for Si–O_t in I01 is 1.02, and the bond length is 1.64 Å, which is much longer than that of the Si=O double bond in a SiO_2 molecule (1.52 Å at the same computational level). All these results indicate that the bond between Si and O_t is a single bond, and that the O_t has radical character and can be denoted as $O_t^{\bullet}$. The NBO (natural bond orbital) charge on the $Si(O_b)_2O_t^{\bullet}$ moiety is +0.96 |e| (O_b denotes the bridging oxygen atom in this study; the charge on each O_b is divided by 2), so we can describe this moiety as $[Si(O_b)_2O_t^{\bullet}]^+$. In the most stable isomer of $V_2Si_2O_9^+$ (I06), $O_t^{\bullet}$ with a spin density of 0.97 |e| exists in the $Si(O_b)_3O_t^{\bullet}$ moiety, of which the NBO charge is 0.46 |e|. The bond order and length of Si–$O_t^{\bullet}$ in I06 are 0.95 and 1.65 Å, respectively. The $O_t^{\bullet}$ radicals in the most stable isomers of $V_2Si_3O_{11}^+$ (I11) and $V_2Si_4O_{13}^+$ (I16) are similar to that in I06. In $V_4SiO_{12}^+$ (I21), the distribution of the radicals is a little complicated. The spin density is located on two terminal oxygen atoms (0.72 |e| on each O_t) and the V atom (−0.44 |e|) bonded with the two O_t atoms. The bond length of V–O_t is 1.64 Å, which is longer than the V=O_t bond (1.56 Å) in the $V(O_b)_3O_t$ moiety of the same isomer. The type of spin density distribution in $V_4SiO_{12}^+$ (I21) may be simply described as $V(O_b)_2(O_tO_t)^{\bullet}$, in which the notation $(O_tO_t)^{\bullet}$ indicates spin density values of about one unit |e| over two terminal oxygen atoms. The NBO charge on the $V(O_b)_2(O_tO_t)^{\bullet}$ moiety is 0.01 |e|. Note that only one O_t atom has the highest spin density values ($\approx$1 |e|) in each of $V_2SiO_7^+$ (I01), $V_2Si_2O_9^+$ (I06), $V_2Si_3O_{11}^+$ (I11), and $V_2Si_4O_{13}^+$ (I16). The singly-occupied molecular orbitals (SOMOs; the MOs are the Kohn–Sham orbitals in DFT) of the five most stable isomers (I01, I06, I11, I16, and I21) are also shown in Figure 3. It can be seen that all the SOMOs are localized on one or two terminal oxygen atoms, which is consistent with the spin density distributions discussed above, and all the SOMOs have the character of oxygen 2p

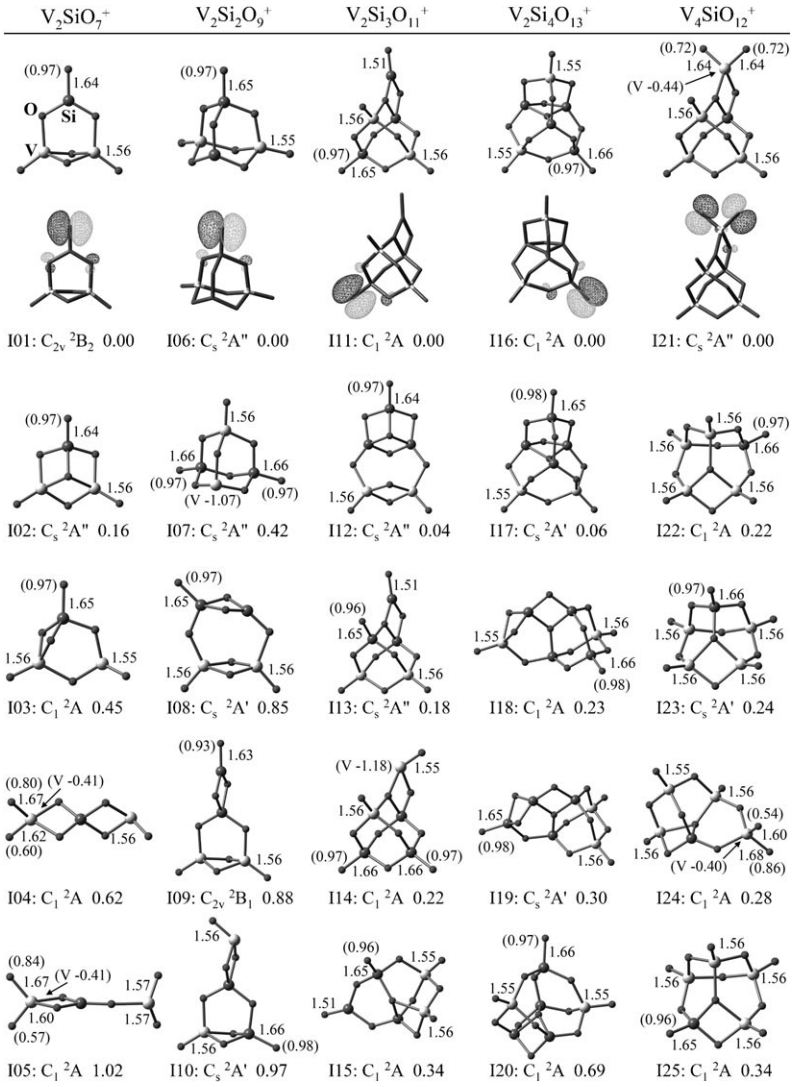

Figure 3. B3LYP/TZVP-calculated stable isomers of $[(V_2O_5)_n(SiO_2)_m]^+$ ($n=1$, $m=1$–4; $n=2$, $m=1$) clusters. The five isomers with the lowest energies are shown for each cluster. The symmetry, electronic state, and energy (in eV) with respect to the most stable isomer are given below each geometry. Bond lengths of V–O_t and Si–O_t are given in Å. Mulliken spin density values greater than 0.4 |e| are given in parentheses for O_t unless specified for V. The SOMOs of the most stable isomers are also given.

orbitals. Thus, all five most stable isomers have $O_t^{\bullet}$, which may be very reactive toward CH_4 activation.

Figure 4 plots the potential energy profiles for the reactions of CH_4 with the most stable isomers of the stoichiometric clusters $[(V_2O_5)_n(SiO_2)_m]^+$ (i.e., I01, I06, I11, I16, and I21). One H atom can transfer from CH_4 to the oxide clusters directly without any barriers, and the association products $[(V_2O_5)_n(SiO_2)_mH]^+\cdots CH_3$ are produced exothermally with ΔH_{0K} values of −1.43, −1.29, −1.25, −1.17, and −0.95 eV for I01, I06, I11, I16, and I21 reaction systems, respectively. Small energies (0.31, 0.22, 0.20, 0.17, and 0.29 eV) are then needed to release the CH_3 radical and form the experimentally observed $[(V_2O_5)_n(SiO_2)_mH]^+$.

The energy released in the formation of $[V_2O_5(SiO_2)_mH\cdots CH_3]^+$ or $[V_2O_5(SiO_2)_mH]^+ + CH_3$ decreases when m increases from 1 to 4. This tendency is consistent with the cluster-size-dependent reactivity observed experimentally, in that a more stable product leads to higher reactivity and vice versa. It is noticeable that RRK (Rice–Ramsperger–Kassel) theory[61] predicts slower unimolecular dissociation for a larger system than for a smaller one, given that the dissociation barrier (or energy) and the total energy that can be used to overcome the barrier are similar. However, this RRK mechanism may not be used to explain the experimentally observed size-dependent rate constants for $[V_2O_5(SiO_2)_m]^+ + CH_4$ ($m=1$–4), because the rates of dissociation $[V_2O_5(SiO_2)_mH\cdots CH_3]^+ \rightarrow [V_2O_5(SiO_2)_mH]^+ + CH_3$ are all in the order of 10^9–10^{10} s^{-1} (see Table S1 in the Supporting Information for details), whereas the collision rate for the clusters with the bath gas (≈300 Pa He) is of the order of 10^7–10^8 s^{-1}. As a result, once $[V_2O_5(SiO_2)_mH\cdots CH_3]^+$ is formed, the possibility of dissociation into separated products ($[V_2O_5(SiO_2)_mH]^+ + CH_3$) is very high (≈100%). We thus suggest that the barrierless C–H bond cleavage step $[V_2O_5(SiO_2)_m]^+ + CH_4 \rightarrow [V_2O_5(SiO_2)_mH\cdots CH_3]^+$ determines the size-dependent reactivity. A steeper potential energy surface (PES) for the C–H bond cleavage means a greater possibility of reaction for each collision between $[V_2O_5(SiO_2)_m]^+$ and CH_4. The DFT-computed energetics in Figure 4 do suggest that the gradients of the PESs for C–H bond cleavage correlate exactly with the reactivity observed experimentally for both $[V_2O_5(SiO_2)_{1-4}]^+$ and $[(V_2O_5)_2SiO_2]^+$ clusters. It is noticeable that, unlike each of the $[V_2O_5(SiO_2)_m]^+$ ($m=1$–4) clusters, in which the spin density is localized on one $O_t^{\bullet}$ atom bonded with Si, in the most stable isomer of $V_4SiO_{12}^+$ the spin density is distributed as $V(O_tO_t)^{\bullet}$. Comparing with $[V_2O_5(SiO_2)_m]^+$, the less localized spin density in $V_4SiO_{12}^+$ leads to less overlap between the reacting O 2p orbital and the CH σ orbital.[34] This is consistent with the DFT flattest PES for the C–H bond cleavage over $V_4SiO_{12}^+$ (Figure 4), and the lowest experimental reactivity of this cluster among $[(V_2O_5)_n(SiO_2)_m]^+$ ($n=1$, $m=1$–4; $n=2$, $m=1$).

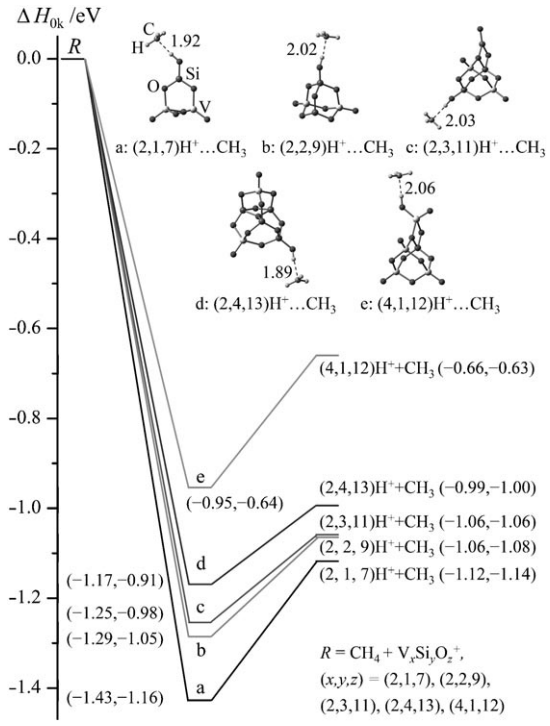

Figure 4. B3LYP/TZVP-calculated reaction pathways for $CH_4+[(V_2O_5)_n(SiO_2)_m]^+ \rightarrow CH_3+[(V_2O_5)_n(SiO_2)_mH]^+$ ($n=1$, $m=1$–4; $n=2$, $m=1$). Association products $V_xSi_yO_zH^+\cdots CH_3$ are denoted as $(x,y,z)H^+\cdots CH_3$, and labeled as a, b, c, d, e, respectively. Distances between the C atom and the abstracted H atom are given in Å. The relative zero-point vibration corrected energy (ΔH_{0K} in eV) and Gibbs free energy at 298 K (ΔG_{298K} in eV) are given in parentheses as (ΔH_{0K}, ΔG_{298K}).

Note that the relative energies of isomers I02, I12, I13, and I17 with respect to the corresponding most stable isomers are less than 0.2 eV. Considering the uncertainties of DFT calculations, these isomers may also be candidates for the ground-state structures, so reactions of CH_4 with these isomers are also calculated by the DFT method. It is found that these isomers also have the active sites of $O_t^{\bullet}$, and the hydrogen-abstraction reaction paths are also overall exothermic and barrierless. The calculated IR spectra for all the stable isomers with relative energies within 0.20 eV are plotted in Figure S1 to be compared with future experimental results.

The DFT calculations are also performed on the nonstoichiometric cluster $V_2Si_2O_{11}^+$, which is also found to be able to abstract one H from CH_4 in our experiments. The most stable structure of $V_2Si_2O_{11}^+$ can be considered to be formed by association of the most stable structure of $V_2Si_2O_9^+$ (I06 in Figure 3) with an O_2 molecule adsorbed in end-on orientation on the threefold-coordinated Si atom (i.e., a superoxide structure Si-O-O). The adsorption energy of O_2 on $V_2Si_2O_9^+$ is 0.80 eV, and the bond length of Si–O_2 is quite long (1.96 Å). The adsorption of O_2 does not change the properties of $O_t^{\bullet}$ in $V_2Si_2O_9^+$ moiety significantly, which leads to the similar reactivities of $V_2Si_2O_{11}^+$ and $V_2Si_2O_9^+$, in agreement with experiment.

Bonding properties of $[(V_2O_5)_n(SiO_2)_m]^+$ clusters: Apart from the five lowest-energy stable isomers for each cluster shown in Figure 3, Figures S2–S6 in the Supporting Information plot the results for isomers (SIn, $n=1$–81) with relative energies within 1.5 eV of those of the most stable structures. Doublet states are found to be more stable than the quartet states for all of the isomers. Spin contaminants are all negligible, with only a few exceptions discussed later.

As mentioned above, in the most stable isomers the oxygen-centered radicals may exist in three types of moieties: $[Si(O_b)_2O_t^{\bullet}]^+$ (I01), $Si(O_b)_3O_t^{\bullet}$ (I06, I011, and I16), and $V(O_b)_2(O_tO_t)^{\bullet}$ (I21). Note that for $V(O_b)_2(O_tO_t)^{\bullet}$ the spin density on the two O_t atoms can be different. For example, in I04, one of the V–O_t bond lengths is significantly longer than the other, and there is more spin density over the O_t atom with the larger V–O_t bond length. As there is one unpaired electron in the 2p orbital of the $O_t^{\bullet}$ atom and the free O^- system has the same electronic structure, $O_t^{\bullet}$ represents an O^- ion. Similarly, $(O_tO_t)^{\bullet}$ can be taken as a mix of one O^{2-} (the double-bonded terminal oxygen atom) with one O^-. For the case in which V and Si are in their highest valence states, in addition to $[Si(O_b)_2O_t^{\bullet}]^+$, $Si(O_b)_3O_t^{\bullet}$, and $V(O_b)_2(O_tO_t)^{\bullet}$, four more moieties may also contain $O_t^{\bullet}$: $[VO_b(O_tO_t)^{\bullet}]^+$, $[V(O_b)_3O_t^{\bullet}]^+$, $V(O_b)_4O_t^{\bullet}$, and $SiO_b(O_tO_t)^{\bullet}$. From Figure 3 and Figures S2–S6 in the Supporting Information, one can see that all of the isomers contain $O_t^{\bullet}$ radicals, and most of the $O_t^{\bullet}$ radicals exist as in the former three types of $O_t^{\bullet}$ moieties. There are only two exceptions for $V_4SiO_{12}^+$ isomers (Figure S6 in the Supporting Information) with relatively high energies: SI63 (0.93 eV) with $[VO_b(O_tO_t)^{\bullet}]^+$ and SI77 (1.33 eV) with $[V(O_b)_3O_t^{\bullet}]^+$. Thus, in the low-lying isomers of $[(V_2O_5)_n(SiO_2)_m]^+$, oxygen-centered radicals bonded with the Si atom (denoted as $SiO_t^{\bullet}$) tend to be in the form of $[Si(O_b)_2O_t^{\bullet}]^+$ or $Si(O_b)_3O_t^{\bullet}$, whereas the ones bonded with the V atom are usually in the form of $V(O_b)_2(O_tO_t)^{\bullet}$ and may be denoted as $V(O_tO_t)^{\bullet}$. Because the radicals are localized and delocalized in $SiO_t^{\bullet}$ and $V(O_tO_t)^{\bullet}$, respectively, one may conclude that oxygen-centered radicals bonded with Si have higher reactivity than those with V for the heteronuclear oxide clusters. Note that in homonuclear V oxide clusters, such as $V_4O_{10}^+$, radicals are localized and exist as $[V(O_b)_3O_t^{\bullet}]^+$, for which the reactivity toward methane may be similar to that of $[Si(O_b)_2O_t^{\bullet}]^+$ in $V_2SiO_7^+$ or $Si(O_b)_3O_t^{\bullet}$ in $V_2Si_2O_9^+$.

The neutral V_2SiO_7 (or $V_2O_5SiO_2$) with the I01 structure (Figure 3) is a closed shell system in which all the atoms are in their highest valence states. It has one Si=O_t and two V=O_t double bonds. The highest occupied molecular orbital (HOMO) of V_2SiO_7 with the I01 structure is located mainly on the 2p orbital of O_t in Si=O_t (rather than that in V=O_t) according to our DFT calculations, which is consistent with the SOMO distributions of $V_2SiO_7^+$ (I01). This situation is similar in most of the other neutral $(V_2O_5)_n(SiO_2)_m$ cluster isomers, in which the HOMO is mostly distributed on the SiO_t site rather than the VO_t site, and in the cluster cations the radicals tend to be in the form of $SiO_t^{\bullet}$ rather than $VO_t^{\bullet}$. Of the 25 isomers in Figure 3 there are only four structures

with $VO_t^{\bullet}$ (I04, I05, I21, and I24) in which there is only one Si atom and no O_t atoms are bonded with the Si atom. For $[(V_2O_5)(SiO_2)_m]^+$ ($m=1$–4) clusters, the most stable isomers are with $SiO_t^{\bullet}$. For $V_4SiO_{12}^+$, in which there is only one Si atom and the molar ratio of V to Si is large, the most stable isomer (I21) is with $VO_t^{\bullet}$, but I22 with $SiO_t^{\bullet}$ is only 0.22 eV higher in energy. Note that the hydrogen atom abstraction from CH_4 by I22 ($\Delta H_{0K}=-0.99$ eV) is more exothermic than that by I21 ($\Delta H_{0K}=-0.66$ eV, see Figure 4).

Recently, we found that in the bimetallic oxide cluster $AlVO_4^+$, the oxygen-centered radical is bonded with Al rather than V.[42] This work indicated that, in most of our tests, in V–Si heteronuclear oxide cations the oxygen-centered radical bonded with Si is not only more reactive (from the view of the localization of radicals), but also more stable, than the one bonded with V. In the condensed-phase catalysis, vanadium oxides are usually supported on various support materials such as SiO_2 and Al_2O_3. It has been pointed out that the reactions on surfaces usually occur at specific active sites[62–64] that involve only a few atoms and may have similar structural and electronic properties to gas-phase clusters. Therefore, our results indicate that the components directly involved with main group metal (e.g., Al) or even nonmetal (e.g., Si) elements, which had usually been considered as support material, can be excited (for example by charge transfer or by photon irradiation) to have radical characters, and could participate directly in surface C–H activation.

It should be pointed out that the low-lying isomers, such as I07 and I14 in Figure 3 (and Figures SI14, SI27, SI28, SI36, and SI52 in the Supporting Information), have the character of multiradicals (MR). In these MR-containing clusters there are two $Si(O_b)_3O_t^{\bullet}$ moieties with spin densities of $+1$ $|e|$ on each $O_t^{\bullet}$, and one V atom with spin density of -1 $|e|$ (or $+1$ $|e|$ in the quartet state). The calculated doublet states are with spin contaminants (the values of $\langle S^2\rangle$ are around 1.75). The energies of the quartet state are found to be higher than or equal to those of the doublet state, but the differences are within 0.003 eV, and their geometric structures are almost identical. In these MR structures, one V atom with spin density of about -1 $|e|$ is in the $+4$ valence state. It is noticeable that some MR isomers are quite stable (e.g., I14 is only 0.22 eV higher in energy than the most stable isomers of $V_2Si_3O_{11}^+$). This indicates that in addition to V in the $+5$ valence state, V in its $+4$ valence state is also quite stable in these stoichiometric heteronuclear oxide clusters, and the multivalence states of vanadium are likely to exist in V_2O_5/SiO_2 materials.

Apart from the moieties that contain $O_t^{\bullet}$, other building blocks with all atoms being in their highest valence states can be written as: $V(O_b)_3O_t$ (e.g., in I01), $VO_b(O_t)_2$ (I05), $V(O_b)_4^+$ (SI02), $V(O_b)_2O_t^+$ (I04), $Si(O_b)_4$ (I11), $Si(O_b)_2O_t$ (I11), $Si(O_b)_3^+$ (I06), and $SiO_bO_t^+$. From the structures obtained by DFT calculations, it can be concluded that isomers with $VO_b(O_t)_2$, $V(O_b)_4^+$, or $SiO_bO_t^+$ are not stable or have high energy, and may be avoided when constructing the stable structures of stoichiometric V–Si heteronuclear oxide clusters. It is interesting to note that the existence of threefold-coordinated oxygen in the heteronuclear clusters (e.g., in the most stable isomers of $V_2Si_3O_{11}^+$, $V_2Si_4O_{13}^+$ and $V_4SiO_{12}^+$ as I11, I16, and I21, respectively) is quite common, whereas such oxygen atoms rarely occur in the most stable structures of the homonuclear vanadium[65–69] or silicon[70–72] oxide clusters.

Conclusion

V–Si heteronuclear oxide cluster cations have been prepared and reacted with CH_4 in a fast-flow reactor. Hydrogen abstraction reactions have been identified over stoichiometric clusters $[(V_2O_5)_n(SiO_2)_m]^+$ ($n=1$, $m=1$–4; $n=2$, $m=1$). The most stable isomers of these stoichiometric clusters are obtained by DFT calculations. Terminal-oxygen-centered radicals ($O_t^{\bullet}$) are found in all of the stable isomers. These $O_t^{\bullet}$ radicals are active sites of the clusters in their reaction with CH_4. The $O_t^{\bullet}$ radicals in $[V_2O_5(SiO_2)_{1-4}]^+$ clusters are bonded with Si rather than V atoms. All the hydrogen abstraction reactions are calculated to be favorable both thermodynamically and kinetically. The suggested building blocks for the stoichiometric heteronuclear oxide clusters cations are $[Si(O_b)_2O_t^{\bullet}]^+$, $Si(O_b)_3O_t^{\bullet}$, and $V(O_b)_2(O_tO_t)^{\bullet}$, together with $V(O_b)_3O_t$, $V(O_b)_2O_t^+$, $Si(O_b)_4$, $Si(O_b)_2O_t$, and $Si(O_b)_3^+$. The threefold-coordinated oxygen atoms exist in some of the clusters. Most of the V atoms are in $+5$ valence state, but in the low-lying energy isomers with multiradical structures one of the V atoms is in the $+4$ state.

This work has revealed the unique structure/property relationship of metal/nonmetal heteronuclear oxide clusters, and provided new insights (such as $Si-O_t^{\bullet}$ rather than $V-O_t^{\bullet}$ active sites, multivalence states of V) into CH_4 activation on silica-supported vanadium oxide catalysts.

Experimental Section

Experimental details: The experimental setup for generation, reaction, and detection of the cationic clusters was similar to that described in previous studies,[34,58,73,74] and only a brief description is given below. The $V_xSi_yO_z^+$ clusters were generated by laser ablation (532 nm Nd:YAG, 5–8 mJ/pulse, 10 Hz) of a rotating and translating V/Si mixed sample [V (99.5%) and Si (99.999%) powders purchased from Alfa Aesar; molar ratio of V:Si = 1:1] in the presence of about 1% O_2 seeded in a pulsed carrier gas (He) with backing pressure of 5 atm. The clusters formed in a narrow channel (2 mm diameter × 25 mm length) were then expanded and reacted with the reactant gases (pure or He-diluted CH_4 or CD_4) in a fast-flow reactor (6 mm diameter × 60 mm length). The reactant gases with backing pressures of about 1–20 kPa were pulsed into the reactor at a position 20 mm downstream from the exit of the cluster formation channel. To eliminate the formation of undesirable hydroxo species, the generation gases (O_2/He) and reactant gases were passed through two 10 m copper tube foils at low temperature ($T=77$ K and 190–240 K, respectively) before they entered the pulsed valves. After reacting in the fast flow reactor, the reactant and product ions exiting from the reactor were skimmed (3 mm diameter) into a vacuum system of a TOF mass spectrometer. Ion signals were generated by averaging 500–1000 traces of independent mass spectra (each corresponding to one laser shot). The

uncertainty of the reported relative ion signals was about 10%. The mass resolution was about 400–500 ($M/\Delta M$) with the current experimental setup. The oxide clusters exiting the cluster formation channel were usually rotationally cold ($T_{rot} \approx 50$ K) and vibrationally hot (T_{vib} can be up to 700 K).[75] The bath gas temperature was around 300–400 K, considering that the carrier gas could be heated during the process of laser ablation. The intracluster vibrations were probably equilibrated close to the bath gas temperature before reacting with the reactant molecules.[34] In our experiments, the instantaneous total gas pressure in the fast-flow reactor was estimated to be around 300 Pa at $T = 350$ K.[58]

Computational details: DFT calculations were performed using the Gaussian 03 program[76] with the B3LYP exchange-correlation functional[77,78] and all-electron polarized triple-ζ valence basis sets (TZVP).[79] This level of theory has been demonstrated by many groups to give reasonably good results with moderate computational cost for the structural properties and energetics of vanadium oxides,[53,65,80–84] and has been widely used in studying the reactions of hydrocarbons on silica-supported vanadia with cluster models.[36,51–54] Geometry optimizations were performed with full relaxation of all atoms and all possible spin multiplicities. Vibrational frequency calculations were performed to check that all the stable isomers had no imaginary frequency. All of the energies reported in this study include zero-point vibrational energy corrections. To study the bonding properties, natural bond orbital (NBO) analyses[85] were performed using NBO 3.1 implemented in Gaussian 03. Cartesian coordinates, electronic energies, and vibrational frequencies for all the optimized structures are available upon request. To obtain reliable global minima for the stoichiometric clusters $[(V_2O_5)_n(SiO_2)_m]^+$, the geometry optimizations were performed starting from a high number of possible candidate structures (more than 200 for each cluster) generated from a systematic search based on the topological structures, and also a simplified basin-hopping method,[86] the details of which are described in the Supporting Information. Further computations using special methods, such as the strict basin-hopping method or genetic algorithm,[20,87,88] may be necessary to confirm that our search was sufficient to obtain the global minima.

Acknowledgements

This work was supported by the Chinese Academy of Sciences (Hundred Talents Fund), the National Natural Science Foundation of China (Nos. 20703048, 20803083, and 20933008), CMS Foundation of the ICCAS (No. CMS-LX200902), the 973 Program (No. 2006CB932100), and the project sponsored by the Scientific Research Foundation for Returned Overseas Chinese Scholars, State Education Ministry.

[1] D. H. R. Barton, *Aldrichimica Acta* **1990**, *23*, 3–10.
[2] H. Schwarz, *Angew. Chem.* **1991**, *103*, 837–838; *Angew. Chem. Int. Ed. Engl.* **1991**, *30*, 820–821.
[3] B. A. Arndtsen, R. G. Bergman, T. A. Mobley, T. H. Peterson, *Acc. Chem. Res.* **1995**, *28*, 154–162.
[4] B. C. Enger, R. Lødeng, A. Holmen, *Appl. Catal. A* **2008**, *346*, 1–27.
[5] J. Roithova', D. Schröder, *Chem. Rev.* **2010**, *110*, 1170–1211.
[6] S. M. Lang, T. M. Bernhardt, R. N. Barnett, U. Landman, *Angew. Chem.* **2010**, *122*, 993–996; *Angew. Chem. Int. Ed.* **2010**, *49*, 980–983.
[7] D. Schröder, *Angew. Chem.* **2010**, *122*, 862–863; *Angew. Chem. Int. Ed.* **2010**, *49*, 850–851.
[8] R. Wesendrup, D. Schröder, H. Schwarz, *Angew. Chem.* **1994**, *106*, 1232–1235; *Angew. Chem. Int. Ed. Engl.* **1994**, *33*, 1174–1176.
[9] M. Diefenbach, M. Bronstrup, M. Aschi, D. Schröder, H. Schwarz, *J. Am. Chem. Soc.* **1999**, *121*, 10614–10625.
[10] M. Pavlov, M. R. A. Blomberg, P. E. M. Siegbahn, R. Wesendrup, C. Heinemann, H. Schwarz, *J. Phys. Chem. A* **1997**, *101*, 1567–1579.
[11] X. G. Zhang, R. Liyanage, P. B. Armentrout, *J. Am. Chem. Soc.* **2001**, *123*, 5563–5575.
[12] D. Schröder, H. Schwarz, *Can. J. Chem.* **2005**, *83*, 1936–1940.
[13] J. N. Harvey, M. Diefenbach, D. Schröder, H. Schwarz, *Int. J. Mass Spectrom.* **1999**, *182–183*, 85–97.
[14] I. Kretzschmar, A. Fiedler, J. N. Harvey, D. Schröder, H. Schwarz, *J. Phys. Chem. A* **1997**, *101*, 6252–6264.
[15] D. Schroeder, A. Fiedler, J. Hrusak, H. Schwarz, *J. Am. Chem. Soc.* **1992**, *114*, 1215–1222.
[16] K. K. Irikura, J. L. Beauchamp, *J. Am. Chem. Soc.* **1989**, *111*, 75–85.
[17] S. Feyel, J. Döbler, D. Schröder, J. Sauer, H. Schwarz, *Angew. Chem.* **2006**, *118*, 4797–4801; *Angew. Chem. Int. Ed.* **2006**, *45*, 4681–4685.
[18] D. Schröder, J. Roithova, *Angew. Chem.* **2006**, *118*, 5835–5838; *Angew. Chem. Int. Ed.* **2006**, *45*, 5705–5708.
[19] S. Feyel, J. Döbler, R. Hoeckendorf, M. K. Beyer, J. Sauer, H. Schwarz, *Angew. Chem.* **2008**, *120*, 1972–1976; *Angew. Chem. Int. Ed.* **2008**, *47*, 1946–1950.
[20] M. Sierka, J. Döbler, J. Sauer, G. Santambrogio, M. Brummer, L. Woste, E. Janssens, G. Meijer, K. R. Asmis, *Angew. Chem.* **2007**, *119*, 3437–3440; *Angew. Chem. Int. Ed.* **2007**, *46*, 3372–3375.
[21] G. de Petris, A. Troiani, M. Rosi, G. Angelini, O. Ursini, *Chem. Eur. J.* **2009**, *15*, 4248–4252.
[22] N. Dietl, M. Engeser, H. Schwarz, *Angew. Chem.* **2009**, *121*, 4955–4957; *Angew. Chem. Int. Ed.* **2009**, *48*, 4861–4863.
[23] Y.-X. Zhao, X.-L. Ding, Y.-P. Ma, Z.-C. Wang, S.-G. He, *Theor. Chem. Acc.* **2010**, DOI: 10.1007/s00214-010-0732-8.
[24] M. Schlangen, H. Schwarz, *Dalton Trans.* **2009**, 10155–10165.
[25] D. Schröder, H. Schwarz, *Proc. Natl. Acad. Sci. USA* **2008**, *105*, 18114–18119.
[26] M. Lersch, M. Tilset, *Chem. Rev.* **2005**, *105*, 2471–2526.
[27] J. H. Lunsford, *Angew. Chem.* **1995**, *107*, 1059–1070; *Angew. Chem. Int. Ed. Engl.* **1995**, *34*, 970–980.
[28] J. H. Lunsford, *Catal. Today* **2000**, *63*, 165–174.
[29] A. A. Fokin, P. R. Schreiner, *Adv. Synth. Catal.* **2003**, *345*, 1035–1052.
[30] J. A. Labinger, *J. Mol. Catal. A* **2004**, *220*, 27–35.
[31] G. I. Panov, K. A. Dubkov, E. V. Starokon, *Catal. Today* **2006**, *117*, 148–155.
[32] M. Chiesa, E. Giamello, M. Che, *Chem. Rev.* **2009**, *110*, 1320–1347.
[33] Y.-X. Zhao, X.-N. Wu, Z.-C. Wang, S.-G. He, X.-L. Ding, *Chem. Commun.* **2010**, *46*, 1736–1738.
[34] X.-N. Wu, Y.-X. Zhao, W. Xue, Z.-C. Wang, S.-G. He, X.-L. Ding, *Phys. Chem. Chem. Phys.* **2010**, *12*, 3984–3997.
[35] I. Muylaert, P. Van Der Voort, *Phys. Chem. Chem. Phys.* **2009**, *11*, 2826–2832.
[36] X.-L. Ding, W. Xue, Y.-P. Ma, Y.-X. Zhao, X.-N. Wu, S.-G. He, *J. Phys. Chem. C* **2010**, *114*, 3161–3169.
[37] M. V. Ganduglia-Pirovano, C. Popa, J. Sauer, H. Abbott, A. Uhl, M. Baron, D. Stacchiola, O. Bondarchuk, S. Shaikhutdinov, H. J. Freund, *J. Am. Chem. Soc.* **2010**, *132*, 2345–2349.
[38] E. Janssens, G. Santambrogio, M. Brummer, L. Woste, P. Lievens, J. Sauer, G. Meijer, K. R. Asmis, *Phys. Rev. Lett.* **2006**, *96*, 233401.
[39] D. W. Rothgeb, E. Hossain, A. T. Kuo, J. L. Troyer, C. C. Jarrold, *J. Chem. Phys.* **2009**, *131*, 044310.
[40] A. Fielicke, K. Rademann, *Chem. Phys. Lett.* **2002**, *359*, 360–366.
[41] M. Nößler, R. Mitrić, V. Bonačić-Koutecký, G. E. Johnson, E. C. Tyo, A. W. Castleman Jr. , *Angew. Chem.* **2010**, *122*, 417–420; *Angew. Chem. Int. Ed.* **2010**, *49*, 407–410.
[42] Z.-C. Wang, X.-N. Wu, Y.-X. Zhao, J.-B. Ma, X.-L. Ding, S.-G. He, *Chem. Phys. Lett.* **2010**, *489*, 25–29.
[43] D. K. Böhme, H. Schwarz, *Angew. Chem.* **2005**, *117*, 2388–2406; *Angew. Chem. Int. Ed.* **2005**, *44*, 2336–2354.
[44] K. A. Zemski, D. R. Justes, A. W. Castleman, *J. Phys. Chem. B* **2002**, *106*, 6136–6148.
[45] T. Waters, G. N. Khairallah, S. Wimala, Y. C. Ang, R. A. J. O'Hair, A. G. Wedd, *Chem. Commun.* **2006**, 4503–4505.
[46] R. A. J. O'Hair, G. N. Khairallah, *J. Cluster Sci.* **2004**, *15*, 331–363.
[47] Y. Gong, M. F. Zhou, L. Andrews, *Chem. Rev.* **2009**, *109*, 6765–6808.
[48] D. Schröder, H. Schwarz, *Top. Organomet. Chem.* **2007**, *22*, 1–15.

[49] L. D. Nguyen, S. Loridant, H. Launay, A. Pigamo, J. L. Dubois, J. M. M. Millet, *J. Catal.* **2006**, *237*, 38–48.
[50] H. Launay, S. Loridant, D. L. Nguyen, A. M. Volodin, J. L. Dubois, J. M. M. Millet, *Catal. Today* **2007**, *128*, 176–182.
[51] X. Rozanska, R. Fortrie, J. Sauer, *J. Phys. Chem. C* **2007**, *111*, 6041–6050.
[52] X. Rozanska, J. Sauer, *Int. J. Quantum Chem.* **2008**, *108*, 2223–2229.
[53] J. Sauer, J. Döbler, *Dalton Trans.* **2004**, 3116–3121.
[54] J. Döbler, M. Pritzsche, J. Sauer, *J. Phys. Chem. C* **2009**, *113*, 12454–12464.
[55] B. M. Weckhuysen, D. E. Keller, *Catal. Today* **2003**, *78*, 25–46.
[56] C. Hess, *ChemPhysChem* **2009**, *10*, 319–326.
[57] J. S. Coursey, D. J. Schwab, R. A. Dragoset, Atomic Weights and Isotopic Compositions, v2.4.1, National Institute of Standards and Technology (http://physics.nist.gov/Comp), Gaithersburg, **2005**.
[58] W. Xue, Z.-C. Wang, S.-G. He, Y. Xie, E. R. Bernstein, *J. Am. Chem. Soc.* **2008**, *130*, 15879–15888.
[59] It is noticeable that the absolute rate constants of $CeO_2^+ + C_2H_4 \rightarrow CeO^+ + C_2H_4O$ and $ZrO_2^+ + CH_4 \rightarrow ZrO_2H^+ + CH_3$ in our previous study[34] using the fast-flow reaction experimental setup (the one adopted in this work) agree well (within a factor of two) with those using the FTICR (Fourier transform ion cyclotron resonance) method in independent studies.[13,60] In contrast, $k_1(V_4O_{10}^+ + CH_4)$ using our fast flow reaction experiment[33] is 1.3×10^{-10} cm^3 molecule^{-1} s^{-1}, which is significantly smaller than the value (5.5×10^{-10} cm^3 molecule^{-1} s^{-1}) from the QHQ experiment (Q = quadrupole and H = hexapole) of Feyel and co-workers.[17] The relatively large discrepancy for $k_1(V_4O_{10}^+ + CH_4)$ is due to: 1) the experimental uncertainties, and 2) other factors such as differences in vibrational energy (E_{vib}) and center-of-mass kinetic energy (E_k) of $V_4O_{10}^+$ in different experiments. The $V_4O_{10}^+$ was generated with laser ablation and supersonic expansion in our experiment, but produced with electro-spray ionization in the QHQ experiment. The E_{vib} or the vibrational temperature (T_{vib}) of vanadium oxide cluster cations before the reaction by our experimental setup may not be high (T_{vib} is possibly around 300–400 K) because rare-gas-atom pickup products such as $V_2O_5Ar^+$ and $V_4O_{10}Xe^+$ can be generated if pure Ar or Xe is pulsed into the fast-flow reactor. The E_k for $V_4O_{10}^+$ with CH_4 is 0.08 ± 0.01 eV in our experiment. It may be interesting to check if such rare-gas-atom pickup products can be generated in the QHQ experiment.
[60] C. Heinemann, H. H. Cornehl, D. Schröder, M. Dolg, H. Schwarz, *Inorg. Chem.* **1996**, *35*, 2463–2475.
[61] T. Baer, P. M. Mayer, *J. Am. Soc. Mass Spectrom.* **1997**, *8*, 103–115.
[62] T. Zambelli, J. Wintterlin, J. Trost, G. Ertl, *Science* **1996**, *273*, 1688–1690.
[63] A. T. Bell, *Science* **2003**, *299*, 1688–1691.
[64] J. M. Thomas, *Top. Catal.* **2006**, *38*, 3–5.
[65] S. F. Vyboishchikov, J. Sauer, *J. Phys. Chem. A* **2000**, *104*, 10913–10922.
[66] G. Santambrogio, M. Brummer, L. Woste, J. Döbler, M. Sierka, J. Sauer, G. Meijer, K. R. Asmis, *Phys. Chem. Chem. Phys.* **2008**, *10*, 3992–4005.
[67] E. Jakubikova, A. K. Rappe, E. R. Bernstein, *J. Phys. Chem. A* **2007**, *111*, 12938–12943.
[68] K. R. Asmis, J. Sauer, *Mass Spectrom. Rev.* **2007**, *26*, 542–562.
[69] S. F. Vyboishchikov, J. Sauer, *J. Phys. Chem. A* **2001**, *105*, 8588–8598.
[70] S. T. Bromley, F. Illas, *Phys. Chem. Chem. Phys.* **2007**, *9*, 1078–1086.
[71] S. T. Bromley, M. A. Zwijnenburg, T. Maschmeyer, *Phys. Rev. Lett.* **2003**, *90*, 035502.
[72] R. Q. Zhang, W. J. Fan, *J. Cluster Sci.* **2006**, *17*, 541–563.
[73] S.-G. He, Y. Xie, F. Dong, S. Heinbuch, E. Jakubikova, J. J. Rocca, E. R. Bernstein, *J. Phys. Chem. A* **2008**, *112*, 11067–11077.
[74] W. Xue, S. Yin, X.-L. Ding, S.-G. He, M.-F. Ge, *J. Phys. Chem. A* **2009**, *113*, 5302–5309.
[75] Y. Matsuda, E. R. Bernstein, *J. Phys. Chem. A* **2005**, *109*, 3803–3811.
[76] Gaussian 03, Revision C.02, M. J. Frisch, G. W. Trucks, H. B. Schlegel, G. E. Scuseria, M. A. Robb, J. R. Cheeseman, J. A. Montgomery, Jr., T. Vreven, K. N. Kudin, J. C. Burant, J. M. Millam, S. S. Iyengar, J. Tomasi, V. Barone, B. Mennucci, M. Cossi, G. Scalmani, N. Rega, G. A. Petersson, H. Nakatsuji, M. Hada, M. Ehara, K. Toyota, R. Fukuda, J. Hasegawa, M. Ishida, T. Nakajima, Y. Honda, O. Kitao, H. Nakai, M. Klene, X. Li, J. E. Knox, H. P. Hratchian, J. B. Cross, V. Bakken, C. Adamo, J. Jaramillo, R. Gomperts, R. E. Stratmann, O. Yazyev, A. J. Austin, R. Cammi, C. Pomelli, J. W. Ochterski, P. Y. Ayala, K. Morokuma, G. A. Voth, P. Salvador, J. J. Dannenberg, V. G. Zakrzewski, S. Dapprich, A. D. Daniels, M. C. Strain, O. Farkas, D. K. Malick, A. D. Rabuck, K. Raghavachari, J. B. Foresman, J. V. Ortiz, Q. Cui, A. G. Baboul, S. Clifford, J. Cioslowski, B. B. Stefanov, G. Liu, A. Liashenko, P. Piskorz, I. Komaromi, R. L. Martin, D. J. Fox, T. Keith, M. A. Al-Laham, C. Y. Peng, A. Nanayakkara, M. Challacombe, P. M. W. Gill, B. Johnson, W. Chen, M. W. Wong, C. Gonzalez, J. A. Pople, Gaussian, Inc., Wallingford CT, **2004**.
[77] A. D. Becke, *J. Chem. Phys.* **1993**, *98*, 5648–5652.
[78] C. T. Lee, W. T. Yang, R. G. Parr, *Phys. Rev. B* **1988**, *37*, 785–789.
[79] A. Schafer, C. Huber, R. Ahlrichs, *J. Chem. Phys.* **1994**, *100*, 5829–5835.
[80] M. Pykavy, C. van Wullen, J. Sauer, *J. Chem. Phys.* **2004**, *120*, 4207–4215.
[81] A. Bande, A. Luchow, *Phys. Chem. Chem. Phys.* **2008**, *10*, 3371–3376.
[82] H. B. Li, S. X. Tian, J. L. Yang, *Chem. Eur. J.* **2009**, *15*, 10747–10751.
[83] D. R. Justes, R. Mitric, N. A. Moore, V. Bonacic-Koutecky, A. W. Castleman, Jr., *J. Am. Chem. Soc.* **2003**, *125*, 6289–6299.
[84] F. Dong, S. Heinbuch, Y. Xie, E. R. Bernstein, J. J. Rocca, Z.-C. Wang, X.-L. Ding, S.-G. He, *J. Am. Chem. Soc.* **2009**, *131*, 1057–1066.
[85] NBO Version 3.1, E. D. Glendening, A. E. Reed, J. E. Carpenter, F. Weinhold, **1995**.
[86] D. J. Wales, J. P. K. Doye, *J. Phys. Chem. A* **1997**, *101*, 5111–5116.
[87] D. M. Deaven, K. M. Ho, *Phys. Rev. Lett.* **1995**, *75*, 288.
[88] B. Hartke, *Angew. Chem.* **2002**, *114*, 1534–1554; *Angew. Chem. Int. Ed.* **2002**, *41*, 1468–1487.

Received: May 13, 2010
Published online: September 8, 2010

